JOURNAL OF PROPULSION AND POWER
Vol. 18, No. 5, September–October 2002

Pilot Flame Effects on Gas Jet Flames in Crossflow

Sien-Fong Goh* and S. R. Gollahalli†
University of Oklahoma, Norman, Oklahoma 73019

Flame structure, which includes the radiation power and temperature profiles, soot concentration profiles, and pollutants emissions (NO, NO_x, CO, and CO_2) of propane and propylene gas diffusion flames with and without a hydrogen pilot flame in crossflow is presented. All of the profiles were obtained at a distance of 50% of the total flame length from the burner. The purpose was to investigate the effects of a pilot flame on the structure of flames in crossflow. The fuel was injected vertically into a horizontal airstream through a burner. The flames at nonpiloted conditions were partially or completely detached form the burner. For the piloted flames, hydrogen was added to completely attach the flames to the burner. Experiments were conducted at two different crossflow speeds, 2.68 m/s and 3.58 m/s. The piloted flames, in general, had lower emissions of NO, NO_x, and CO_2. The temperature profiles in all flames showed a peak near the flame center. The pilot flame did not significantly influence the flame temperature profiles at the crossflow speed of 2.68 m/s. However, at 3.58 m/s, the overall flame temperature for both fuels was lower in the piloted flames. The nonpiloted detached flame showed higher concentrations of NO_x, CO_2, and O_2, but had a lower soot concentration. All of the piloted flames appeared to be longer and narrower compared to detached flames. Piloted flames also produced higher radiation, produced more smoke, and appeared more luminous than detached flames.

Introduction

BECAUSE of the important applications of turbulent diffusion flames in crossflow (TDFCF), for instance, flare stacks and industrial furnaces, numerous investigations in this area have been performed. The structure of a TDFCF is complex compared to the structure of a flame in quiescent conditions. The rate of entrainment into flame is enhanced by the crossflow across the path of the incoming jet. Over the last three decades, there were several extensive experimental, empirical, semi-empirical, and analytical studies on the fluid mechanics and reaction kinetics of TDFCF, for example, Bruzustowski,[1] Gollahalli et al.,[2] Gollahalli and Nanjudappa,[3] Broadwell and Bredenthal,[4] and Kalghatgi.[5]

Many industrial and residential applications use pilot flames for flame stabilization or ignition. The knowledge behind the influence of a pilot flame on the overall flame combustion and fluid mechanics characteristics is important. Pilot flames are used in many research studies,[6–9] primarily to keep the flames attached to the burner and to create controlled conditions by avoiding the complexities of air infusion below the flame base. Turns and Myhr[10] performed a study on the pilot flame effects on a turbulent flame in quiescent conditions. In their study, they found that hydrogen pilot flame increased slightly the flame temperature, NO_x emission, flame length, and radiation fraction for CH_4, but decreased them for C_2H_4. They concluded that a pilot flame provided little influence on the overall performance compared to other major factors. Pilot flames are generally used in TDFCF applications. At low crosswinds, the pilot flames are effective in keeping the flame attached over the entire burner rim. However, at high crosswinds, a partial or total detachment of the flame from the burner rim occurs. This change has a marked influence on the rate of cross-stream fluid entry into the base of a TDFCF and, hence, on its combustion and pollution characteristics. Because of the absence of literature on the effects of pilot flames on TDFCF, we initiated the present study.

The objective of the present study was to investigate the effects of a pilot flame on the flame structure and emission characteristics of gas jet flames in crossflow. Specifically, the difference between the totally attached and detached TDFCF was the focus. Two fuels were selected for the study, propane and propylene, because of their widely differing sooting tendencies. Experiments were conducted at two crossflow speeds, 2.68 and 3.58 m/s. Flame temperature; species concentration and soot concentration profiles; flame emission indices of NO, NO_x, CO, and CO_2; and flame radiation were measured.

Experimental Techniques

Experiments were performed in the University of Oklahoma low-speed combustion wind tunnel. The wind tunnel had a contraction ratio of 10. Figure 1 shows a schematic diagram of the dimensions of the wind tunnel. The overall length of the wind tunnel was 1130 cm, and the test section was 250 cm long, 58 cm wide, and 53 cm high. Both sidewalls of the test section were constructed with Pyrex™ plate glass panels for the optical access with the laser (soot concentration measurement) and flame photography. The top and bottom panels of the test-section walls were made of aluminum sheet metal plates with slots to introduce probes and the burner. The burner protruded about 7 cm into the test section from the tunnel floor and was placed perpendicular to the cross stream. The fuel jet was ignited with an electrical lighter, which was placed near the burner and retracted from the ceiling of the test section after ignition of the fuel jet was achieved. The wind tunnel was capable of providing a flow velocity ranging from 1 to 6.5 m/s in the test section. The flow was relatively uniform in the test section except near the walls because of the boundary layer.

The gas supply trains consisted of propane, propylene and hydrogen cylinders, pressure regulators, calibrated rotameters, and manifolds. There were two different gas supply trains, one for hydrocarbon fuels and another for hydrogen. After entering the inlet manifold, the fuel supply was distributed to five rotameters, which were connected in parallel to an exit manifold. At a location just before the gases entered the burner, a K-type thermocouple connected to a digital meter was installed in the line for fuel temperature measurement. The hydrogen line was similar to the hydrocarbon fuel lines, but a single rotameter without a manifold was sufficient. The burners were made of two concentric circular steel tubes. The inner tube with an inside diameter of 6.35 mm was supplied with

Presented as Paper 2000-0592 at the AIAA 38th Aerospace Sciences Meeting and Exhibit, Reno, NV, 10–13 January 2000; received 20 November 2001; revision received 23 April 2002; accepted for publication 1 May 2002.

*Research Assistant, Combustion and Flame Dynamics Laboratory, School of Aerospace and Mechanical Engineering. Student Member AIAA.

†Lesch Centennial Chair, Combustion and Flame Dynamics Laboratory, School of Aerospace and Mechanical Engineering. Associate Fellow AIAA.

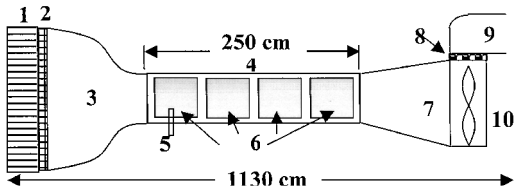

Fig. 1 Combustion wind tunnel: 1, flow straightener; 2, screens; 3, contraction section; 4, test section; 5, burner; 6, pyrex windows; 7, diffuser section; 8, shutter; 9, exhaust; and 10, fan.

hydrocarbon fuels, and the outer tube with an inside diameter of 25 mm was supplied with hydrogen, to produce the pilot flame to keep the hydrocarbon flame attached to the burner. In the annular space between the tubes, fine steel wool was stuffed to provide a uniform flow of hydrogen.

The transverse profiles of temperature, species concentrations, and soot concentration were measured at different locations. The profiles on a section located at 50% of the flame length from the burner are presented here. The temperature was measured with an in-house-made R-type (platinum–platinum 13% rhodium with hot-junction 0.59-mm diam) thermocouple. The output of thermocouple was acquired with a personal computer equipped with an A/D converter at a frequency of 1 kHz and the signals, computer-averaged over 1 s, were recorded. These data were further time-averaged over 2 min to yield long-time mean values.

Soot concentration was measured using a radiation attenuation technique proposed by Yagi and Iino.[11] Soot concentration profiles were also measured at a section located 50% of the flame length from the burner. The measurements were taken using a helium–neon laser with wavelength of 635 nm and power output of 15 mW as the light source. The laser beam passed horizontally through the flame field to the power detector on the other side of the flame. For each measurement, the power incident on the detector with and without flame was recorded. Soot volume fraction was calculated from the attenuation data.

The gas sample from the flame products was collected and analyzed with four different analyzers. Two nondispersive infrared (NDIR) Rosemount Analytical Model 880A analyzers were used for the CO and CO_2 concentration measurements. Oxygen concentration was measured with an MSA Catalyst Research MiniOX I polarographic oxygen analyzer. The NO and NO_x concentrations were measured using a Thermo Environmental Instruments Model 42H chemiluminescent analyzer. The combustion products were collected through a conical duct with an inlet opening of 15 cm. The wall of the cone consisted of several steps to promote mixing of combustion products before the gas samples were collected at the end of the cone using a probe that was connected to the measurement setup. The sampling rate was 12 ml/s, and it was regulated by a flow meter. The sample gas was first chilled to remove moisture and filtered to remove particulate matter before being pumped into the analyzers. The transverse concentration profiles of CO, CO_2, NO, and O_2 were measured with the same instrumentation used for emission measurements. The measurement of flame radiation emission yielded just relative values. An absolute measurement could not be achieved because Pyrex glass windows of the wind tunnel absorbed a part of the radiation. The radiation absorption characteristics of the Pyrex glass could not be quantified accurately for each flame, and, hence, the following procedure was employed to obtain relative effects. First, the readings of the flame radiation passing through Pyrex glass was taken. Then, the flame was turned off and the radiation emitted just from the flame heated Pyrex glass was recorded. The net flame radiation passing through Pyrex glass was estimated by subtracting the second reading from the first reading. A wide-angle (150-deg viewing angle) highly sensitive pyrheliometer of absorptivity 0.96 was used for flame radiation measurement. The radiometer was mounted at approximately the midlength of the flame and far enough (1.5 flame lengths) from the flame axis to satisfy the inverse-square law.

A single lens reflex (SLR) camera with 100 ASA film was used to obtain the flame images with three different shutter speeds (1, 1/125, and 1/250 s). The flame height was taken as the distance from the burner tip to the end of the continuous image of the flame on 1-s exposure photographs. The schematic of overall experimental setup is shown in Fig. 2. Table 1 lists the ranges of experimental conditions and Table 2 lists the experimental uncertainties at 95% confidence level.

Table 1 Experimental conditions

Parameter	Value
Burner	
Fuel tube (i.d.)	6.35 mm
Hydrogen tube (i.d.)	25 mm
Fuel	Propane (purity 90%+)
	Propylene (purity 75%+)
Cross-flow speed	2.68 m/s
	3.85 m/s
Fuel flow rate	
Propane at 2.68 m/s	3.9 kg/h
at 3.58 m/s	3.42 kg/h
Propylene at 2.68 m/s	4.38 kg/h
at 3.58 m/s	4.14 kg/h
Hydrogen flow rate for all piloted flames	8.36×10^{-5} kg/min
Fuel jet reynolds number range	22,500–27,700
Jet/crossflow velocity ratio range	4.71–8.4
Jet/crossflow momentum flux ratio range	32–97

Table 2 Uncertainty level in results (at 95% confident level)

Parameter	Value
Emission	
EI NO, g/kg	0.06
EI NO_x, g/kg	0.20
CO_2, %	0.07
O_2, %	0.06
Species concentration	
NO, ppm	1.33
CO, ppm	0.14
CO_2, %	0.16
O_2, %	0.05
Temperature, K	9.99
Soot, g/ml	$1.86E-05$
Radiation, kW	0.034

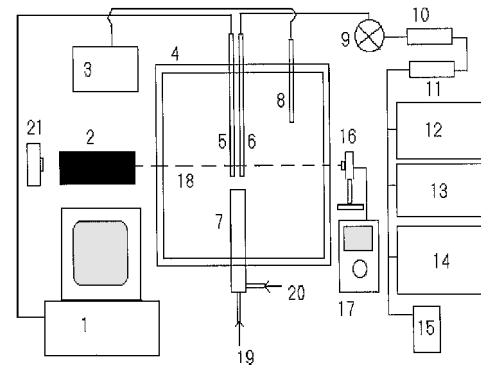

Fig. 2 Schematic of experimental setup: 1, personal computer and data acquisition board; 2, He-Ne laser; 3, electronic manometer; 4, test section of wind tunnel; 5, thermocouple; 6, sample gas collecting probe; 7, burner; 8, pitot-tube; 9, sampling pump; 10, condenser; 11, filter; 12, CO_2 analyzer; 13, CO analyzer; 14, NO_x analyzer; 15, O_2 analyzer; 16, laser power detector; 17, power meter; 18, laser beam; 19, fuel supply; 20, hydrogen supply; and 21, pyrheliometer.

Results and Discussion

Flame Appearance

Flames were longer and narrower for the piloted condition compared to the detached condition, probably due to the lower turbulent

mixing and a reduction of cross-stream air entrainment at the flame base in the presence of the pilot flame. The absence of the pilot flame enhanced the air–fuel mixing in the detached flames. The photographs also showed the piloted flames appeared more luminous, which was an indication of the higher concentration of in-flame soot, which is discussed later. The flame length is defined as the curvilinear distance along the flame centerline from the burner tip to the tip of the contiguous visible flame on a 1-s exposure photograph. The flame lengths are given in Table 3.

Table 3 Flame length

Speed, m/s	Flame length, cm	
	Attached	Piloted
	Propane	
2.68	73.6	63.5
3.58	78.7	73.6
	Propylene	
2.68	81.3	66.0
3.58	86.4	76.2

Emission Analysis

The pollutant emission index results are shown in Tables 4 and 5. The overall observation was that the detached flames emitted higher amount of pollutants, CO, CO_2, NO, and NO_x, although in some cases CO emission indices for piloted flames were higher. The O_2 concentration measured in the exhaust was lower for detached flames. The reasons behind these observations are explained by flame structure measurements. The primary nitrogen oxide from the combustion of a diffusion flame in quiescent condition is NO (Turns[12]). However, in this study, there were large differences between the emission indices of NO and NO_x. Generally, the oxidation of NO to NO_2 becomes significant in low-temperature mixing regions.[12] The intensive mixing of the flame with the cooler surrounding air from the crossflow created a low-temperature mixing region around the flame. Hence, more NO was converted NO_2 in a TDFCF than quiescent conditions.

Flame Structure

Far Burner Transverse Profiles

Temperature profiles. The measured temperature profiles at all flame conditions showed approximately the same trend, where the maximum temperature was located at the center of the flame. The temperature profiles are shown in Fig. 3. In Figs. 3, r represents the transverse vertical location from the centerline of the flame, and it is normalized with burner inside diameter d. The maximum flame temperature for both propane and propylene at both conditions (with and without the pilot flame) at 2.68 m/s crossflow speed was around 1700 K, but there were significant differences at 3.58 m/s crossflow speed. At 3.58 m/s, the detached flame had a higher peak flame temperature; the propane detached flame had a peak temperature

Table 4 Emission indices and exhaust concentration, piloted flame

Speed, m/s	*EI* NO, g/kg	*EI* NO_x, g/kg	*EI* CO, g/kg	CO_2, mole %	O_2, mole %
		Propane			
2.68	2.63	4.1	9.87	1.32	18.5
3.58	1.64	2.66	3.69	1.46	18
		Propylene			
2.68	2.31	3.59	8.88	1.62	18.3
3.58	2.64	4.18	9.37	1.28	18.4

Table 5 Emission indices and exhaust concentration, detached flame

Speed, m/s	*EI* NO, g/kg	*EI* NO_x, g/kg	*EI* CO, g/kg	CO_2, mole %	O_2, mole %
		Propane			
2.68	2.65	4.21	8.67	1.04	18
3.58	2.54	4.41	13.3	1.64	17.6
		Propylene			
2.68	2.36	3.68	6.75	1.66	18.2
3.58	3.01	4.39	16.86	1.96	17.1

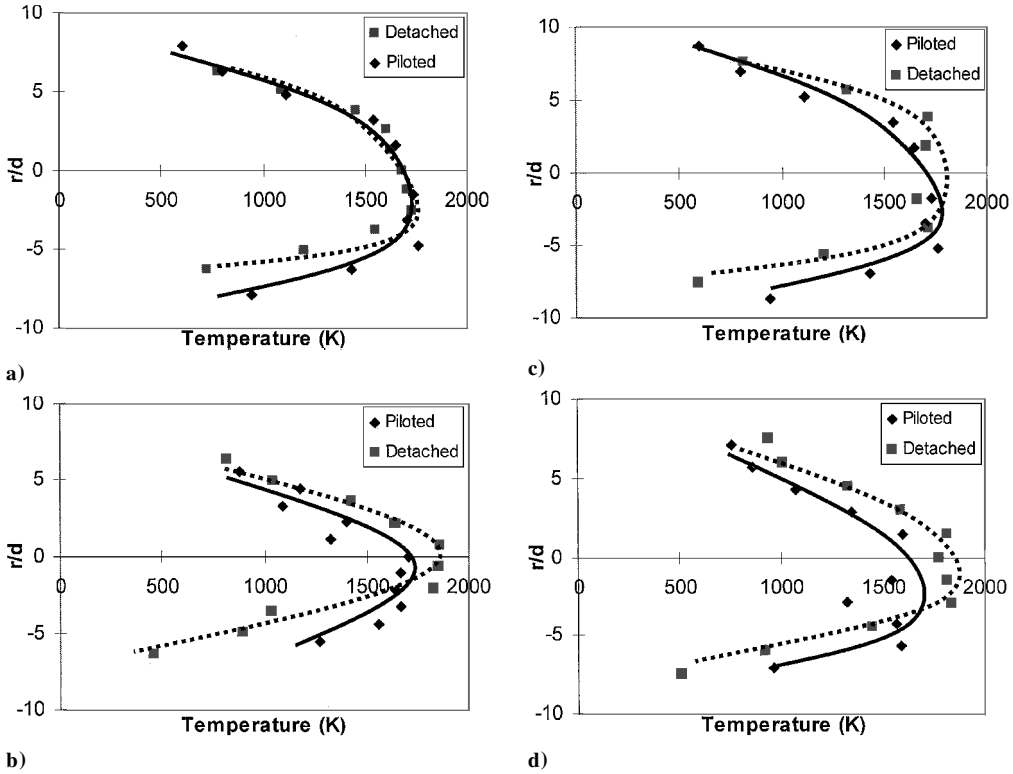

Fig. 3 Transverse temperature profiles at 50% flame length: a) and c) at crosswind velocity of 2.68 m/s and b) and d) at crosswind velocity 3.58 m/s; a) and b) with propane and c) and d) with propylene.

of 1860 K compared the peak temperature of 1710 K in the piloted flame. The corresponding values in the propylene flame were 1810 and 1600 K. The higher temperature in the detached flame indicates a higher oxidation rate, which is reasonable because of a lower O_2 concentration in the exhaust of the detached flame compared with piloted flame. The exhaust concentration results (Tables 4 and 5) showed that the detached flame had a lower O_2 concentration, which indicates that more O_2 had been consumed in the flame. The higher fuel oxidation rate was also indicated by the CO_2 concentration profiles of both fuels, where detached flames had a higher CO_2 concentration compared to piloted flames.

Gaseous species concentration profiles. These concentration profile measurements were performed with the same spatial increments and at the same location employed for temperature measurement. The results at the 50% of the flame length are presented. Overall, the detached flames had higher CO, CO_2, NO, and O_2 concentrations compared to piloted flames. Results for both 2.68 m/s and 3.58 m/s crossflow speeds are shown in Figs. 4 and 5.

The NO emission shown in Tables 4 and 5 was higher in the detached flame, due to the two following reasons: First, the primary NO formation route, thermal mechanism,[12] is strongly coupled with the flame temperature. As discussed in the preceding section, the

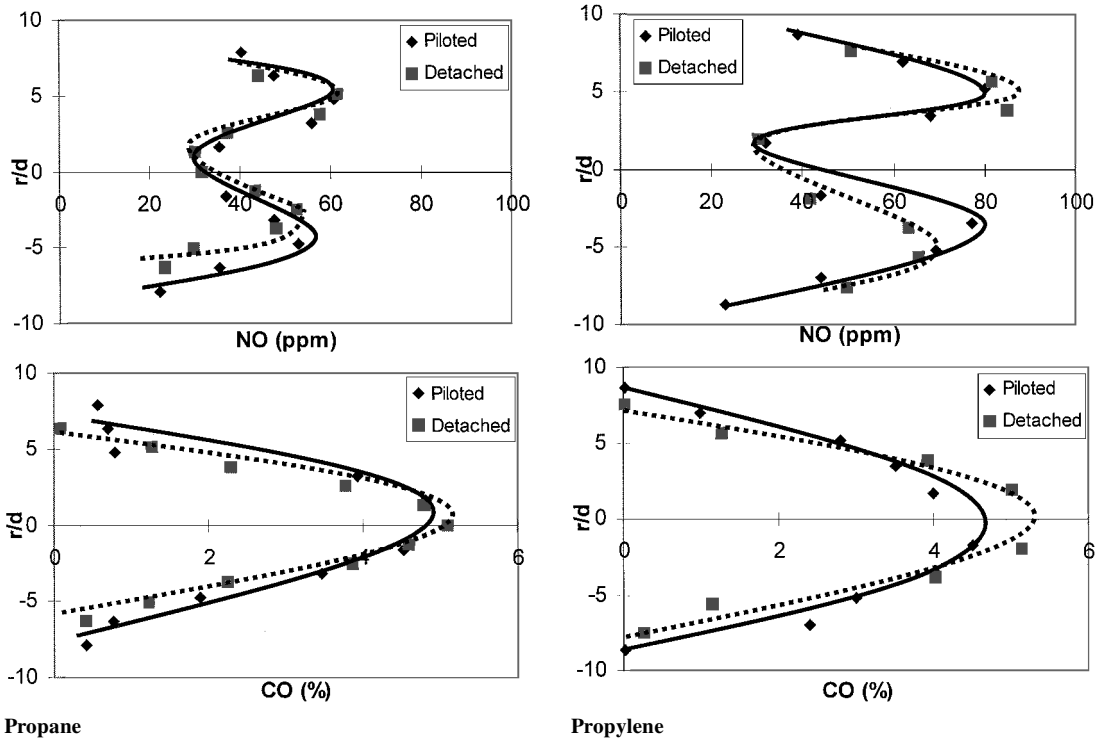

Fig. 4a Transverse concentration profiles of CO and NO at 50% flame length at a crosswind velocity of 2.68 m/s.

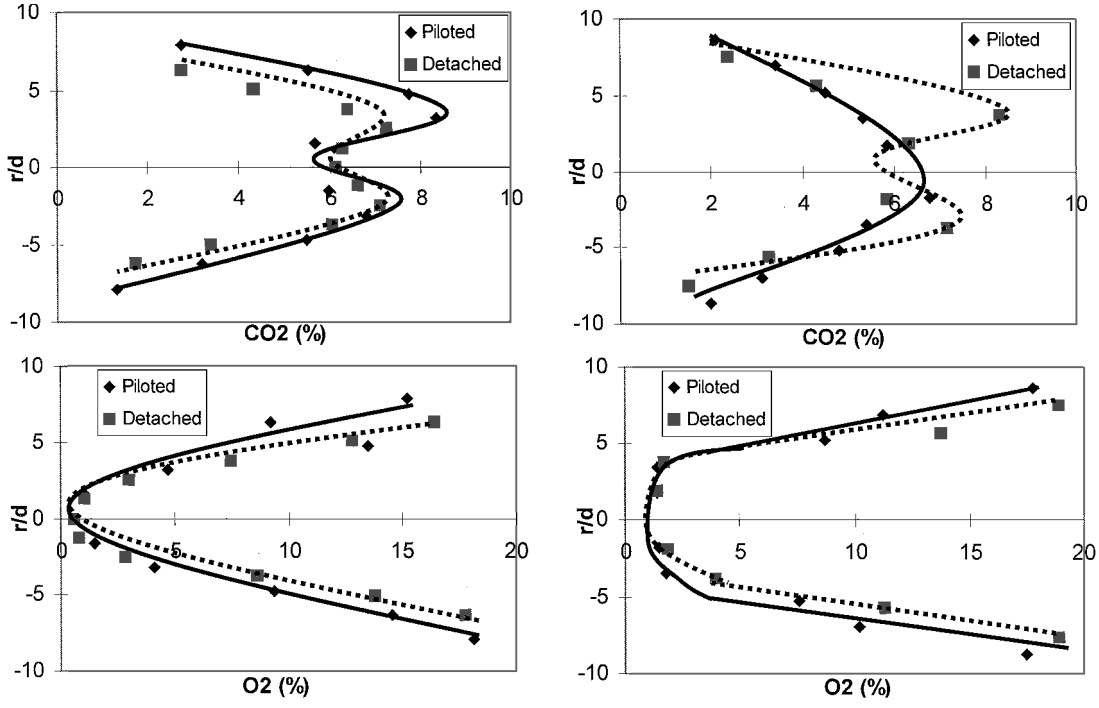

Fig. 4b Transverse concentration profiles of CO_2 and O_2 at 50% flame length at a crosswind velocity of 2.68 m/s.

temperature in the detached flames was higher compared to that in the piloted flame. Second, the NO formation mechanism also depends on the O_2 availability. From the O_2 concentration profiles (Fig. 4), we noticed that the detached flames had a higher in-flame O_2 concentration. The NO concentration profiles show a peak along the transverse direction. While proceeding inward from the crossflow toward the flame centerline, we notice that the temperature increases, so that the NO formation rate also increases. Further proceeding into the flame center region, the O_2 concentration decreases; as a result, the NO formation rate also decreases.

Both the higher temperatures and O_2 concentrations not only promote NO formation, but also play an important role in CO and CO_2 formation. The abundance of O_2 in the detached flames make the soot oxidation process easier compared to that in the pilot flames. Also, it explains why the detached flame had higher CO_2 concentrations. Two other observations that support this explanation are the lower soot concentration and radiation in the detached flame. The higher O_2 concentration in the detached flame is mainly due to the fluid mechanics and the O_2 consumption rate in the flame. The absence of the pilot flame causing the flame detached from the burner created an open area at the flame base where cross-stream air directly enters the flame. The frontal area facing the incoming crossflow increases the air–fuel mixing and makes the flame behave like a premixed flame. We noticed that the O_2 concentration decreases in the flame base region.

Soot concentration profiles. Obtaining a set of smooth profiles without much scatter in soot concentration measurements in a low-sooting turbulent flame was difficult and not repeatable. Propylene, which is a higher soot producing fuel compared to propane, has less scatter in soot concentration measurements. Hence, only propylene results are discussed here, (Fig. 6). As discussed in the preceding

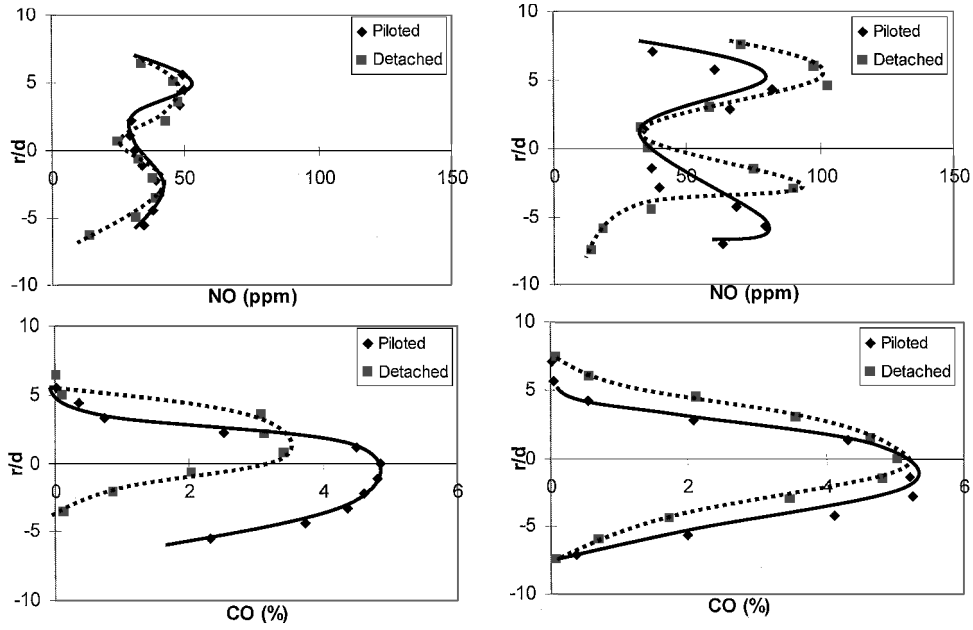

Fig. 5a Transverse concentration profiles of CO and NO at 50% flame length at a crosswind velocity of 3.58 m/s.

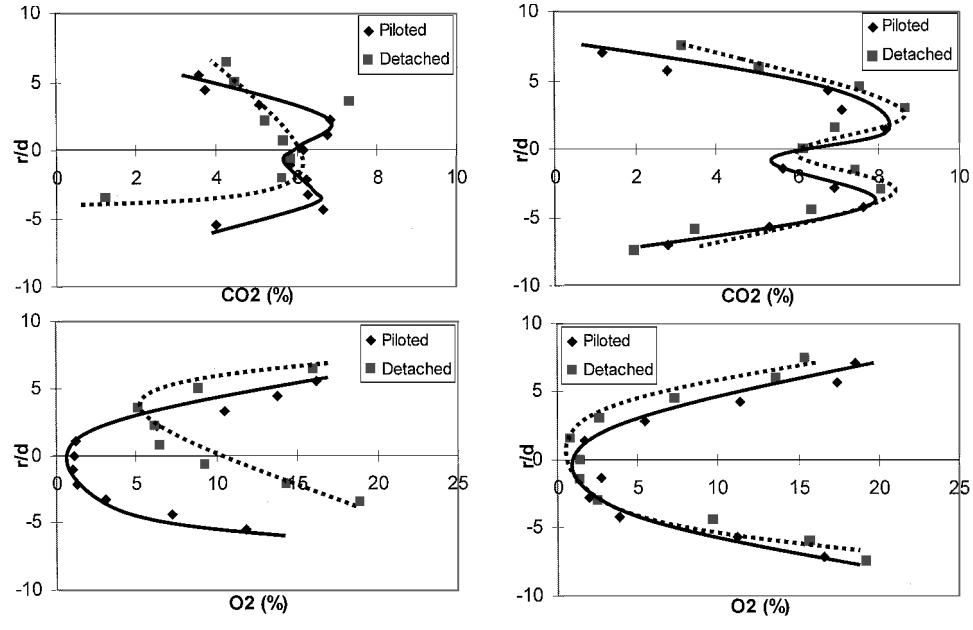

Fig. 5b Transverse concentration profiles of CO_2 and O_2 at 50% flame length at a crosswind velocity of 3.58 m/s.

section, more O_2 enters the detached flames. Hence, soot concentration in the detached flame was lower compared to that in the piloted flame. By comparing soot concentration profiles in the piloted flame and the detached flame, at 2.68 m/s crossflow speed, we notice that the decrease is less significant, but at 3.58 m/s, the peak soot concentration decreased by about half, from 5.5×10^{-7} g/ml to 2.5×10^{-7} g/ml.

Overall, the lower of soot concentration in the detached flame was due to the higher O_2 concentration in the flame causing more soot to oxidize. The concentration profiles on the detached flames were slightly narrower compared to those in the piloted flame. This may be due to the better air–fuel mixing for the detached flame at the outer flame region causing an increase of soot oxidation rate at this region; hence, less soot is present in this region.

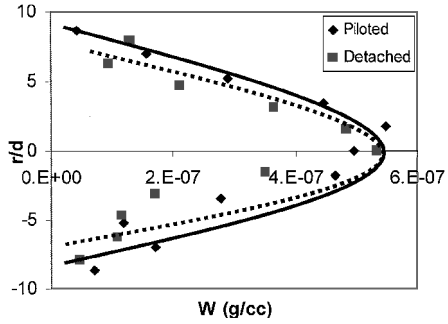

Fig. 6 Transverse soot concentration profiles in propylene flames at a) 2.68 m/s and b) 3.58 m/s.

Flame radiation. As discussed in the instrumentation section, the radiation measurements are satisfactory for only relative comparisons of results obtained at different flame conditions. For all cases, the piloted flames produced higher flame radiation compared to detached flames. Piloted flames had a higher soot concentration because of the lower oxidation rate. The higher soot concentration in piloted flames resulted in a higher continuum radiation from soot. Tables 6 and 7 show the relative radiation results.

Near-Burner Centerline Profiles

The preceding results depict the consequences of pilot flames on the global flame characteristics. To understand the reasons for these observations, we measured the differences in the near-burner flame structure attributable to piloted flames. For simplicity, we recorded

Table 6 Relative radiation results, piloted flame

Crossflow speed, m/s	Fuel	Flame radiation, W
2.68	Propylene	1239.38
2.68	Propane	1085.02
3.58	Propylene	1200.55
3.58	Propane	464.89

Table 7 Relative radiation results, detached flame

Crossflow speed, m/s	Fuel	Flame radiation, W
2.68	Propylene	1138.55
2.68	Propane	807.90
3.58	Propylene	877.53
3.58	Propane	416.45

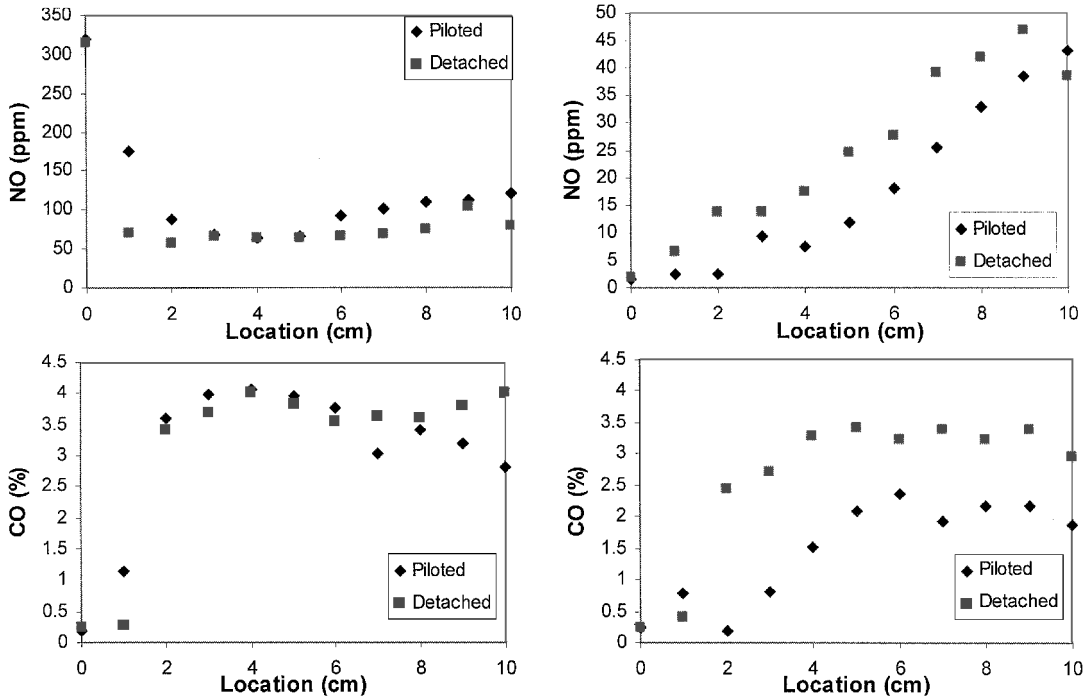

Fig. 7 Centerline concentration profiles of CO and NO at 50% flame length at a crosswind velocity of 2.68 m/s.

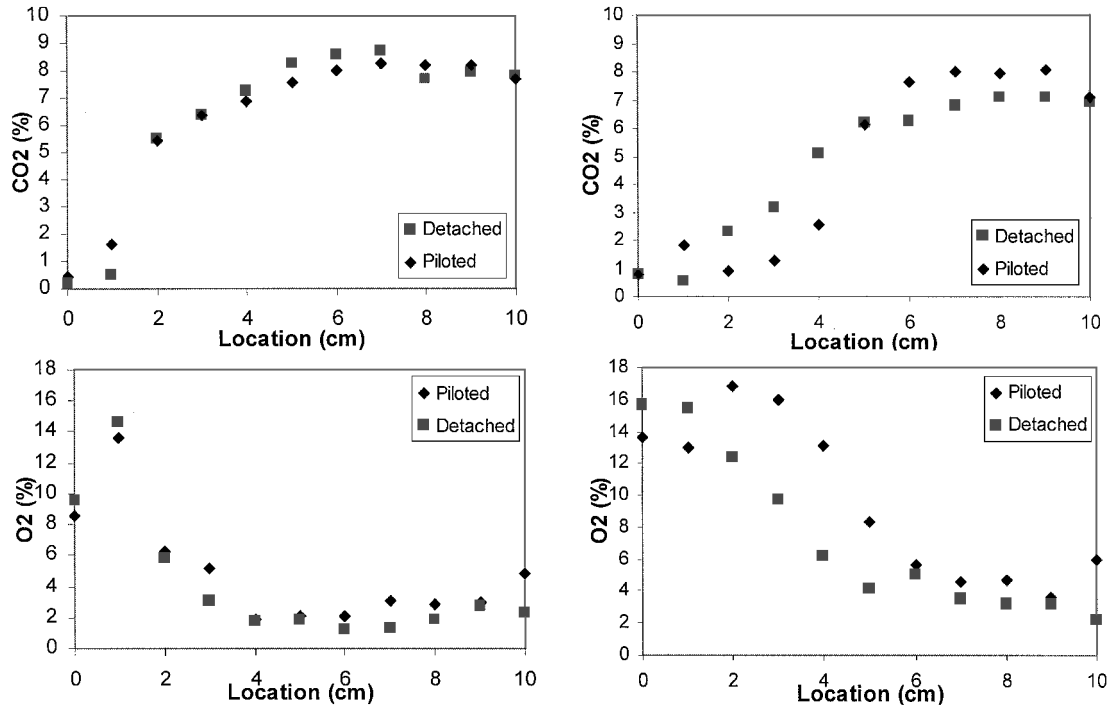

Fig. 8 Centerline concentration profiles of CO_2 and O_2 at 50% flame length at a crosswind velocity of 2.68 m/s.

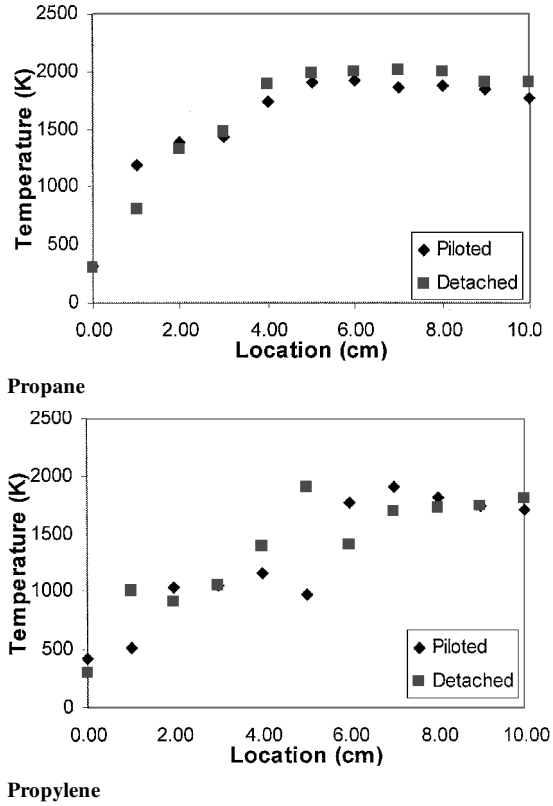

Fig. 9 Centerline temperature profiles in the near-burner region at a crosswind velocity of 2.68 m/s.

the temperature and concentration profiles along the flame centerline up to about 10 cm. The centerline is the line along the crossflow. These profiles show the effects of restricting the crossflow air into the flame base and consequent changes in the flame structure.

Figure 7 shows the differences between piloted and nonpiloted (detached) conditions in the concentration profiles of NO and CO in the jet flames of propylene and propane in crossflow. Figure 8 shows these effects on CO_2 and O_2 profiles, whereas Fig. 9 shows the changes in temperature profiles. We notice that in the propylene flame, the NO concentration is high (about 325 ppm) close to the burner and decreases sharply (about 75 ppm) in a few diameters, then gradually increases (100 ppm) over 10 cm away from the burner. However, in the propane flame the NO concentration is low close to the burner and monotonically increases to about 50 ppm in the same distance. The very high value of NO concentration in the immediate vicinity of the burner in the propylene may be attributed to the high concentration of CH radicals due to the pyrolysis of propylene compared to that of propane, and the consequent increase in HCN related reactions, which contribute to the NO formation. There were two reasons for higher concentration of CH radicals in propylene flame than in propane flame. First, propylene fuel mass flow rate was higher than propane (11.0% by mass higher for 2.68 m/s and 17.4% for 3.58 m/s). Second, propylene fuel is unsaturated. Parts of the steps in propane fuel reaction are from propylene molecules.[13] In the propylene flame, these reactions continue to dominate the thermal NO formation downstream, as noticed by the higher values of NO concentration in piloted flame, which curtail the influx of oxygen into the flame. On the other hand, in the propane flame, where thermal NO is a major component, the higher influx of air in the detached flame results in higher concentrations of NO. The high concentrations of hydrocarbon in the near-burner region of propylene flames, and consequent weak manifestation of the differences between the detached and piloted flames, are noticed in the CO, CO_2, O_2, and temperature profiles. In propane flames, the effects of more oxygen infusion into the detached flames on NO and CO concentration are significant. The effects on CO_2, O_2, and temperature profiles are not conspicuous, particularly in the downstream region. This is due to the much shorter flame of propane compared to the propylene flame, which indicates high levels of mixing and turbulence in the near burner end of flame. Furthermore, the high level of oxygen concentration near the burner in both piloted and detached flames indicates that the pilot flame of hydrogen, although it provides an anchoring point, does not effectively block the infusion of oxygen into the flame base.

Conclusions

Without the pilot flame, the flames were detached and created an open flame base in the near-burner region. This opening allowed more air infusion into the flame. Hence, the combustion

process was supposed to be more efficient, and less pollutants were expected. However, from the emission results, for some of the cases the pollutant indices for the detached flame were higher compared with those in the piloted flame. The detached flames were shorter but wider compared with piloted flames. In the piloted (attached) flames, the cross-stream air flows over the fuel jet fluid and does not penetrate into the flame base. In the detached flames, air enters through the opening created at the flame base, which increases the flame turbulence and radial spreading of the flame. The larger air entrainment enhances fuel burnout rate and increases the emission of NO and NO_x. The piloted flame, on the other hand, produces more smoke due to incomplete combustion.

References

[1]Brzustowski, T. A., "Flaring in the Energy Industry," *Progress in Energy Combustion Science*, Vol. 2, No. 3, 1976, pp. 129–141.

[2]Gollahalli, S. R., Brzustowski, T. A., and Sullivan, H. F., "Characteristic of a Turbulent Propane Diffusion Flame in a Cross Wind," *Transactions of the Canadian Society of Mechanical Engineers*, Vol. 3, No. 4, 1975, pp. 205–213.

[3]Gollahalli, S. R., and Nanjundappa, B., "Burner Wake Stabilized Gas Jet Flame in Cross-Flow," *Combustion Science and Technology*, Vol. 109, Nos. 1–6, 1995, pp. 327–346.

[4]Broadwel, J. E., and Breidenthal, R. E., "Structure and Mixing of Transverse Jet in Incompressible Flow," *Journal of Fluid Mechanics*, Vol. 148, 1984, pp. 405–412.

[5]Kalghatgi, G. T., "The Visible Shape and Size of a Turbulent Hydrocarbon Jet Diffusion Flame in a Cross-Wind," *Combustion and Flame*, Vol. 52, No. 1, Aug. 1983, pp. 91–106.

[6]Starner, S. H., and Bilger, R. W., "Characterstics of a Piloted Diffusion Flame Designed for Study of Combustion Turbulence Interactions," *Combustion and Flame*, Vol. 61, No. 1, July 1985, pp. 29–38.

[7]Peters, T. W. J., Stroomer, P. P. J., DeVries, J. E., Roekarts, D. J. E. M., and Hoogendoorn, C. J., "Comparative Experimental and Numerical Investigation of a Piloted Turbulent Natural-Gas Diffusion Flame," *Twenty-Fifth Symposium (International) on Combustion*, Combustion Inst., Pittsburgh, PA, 1994, pp. 1241–1248.

[8]Barnes, J. C., and Mellor, A. M., "Effects of Unmixedness in Piloted-Lean Premixed Gas-Turbine Combustors," *Journal of Propulsion and Power*, Vol. 14, No. 6, 1998, pp. 967–973.

[9]Starner, S. H., Bilger, R. W., Dibble, R. W., Barlow, R. S., Fourguette, D. C., and Long, M. B., "Joint Planar CH and OH LIF imaging in Piloted Turbulent Jet Diffusion Flames Near Extinction," *Twenty-Fourth Symposium (International) on Combustion*, Combustion Inst., Pittsburgh, PA, 1992, pp. 341–349.

[10]Turns, S. R., and Myhr, F. H., "Oxides of Nitrogen Emissions from Turbulent Jet Flames: Part I—Fuel Effects and Flame Radiation," *Combustion and Flame*, Vol. 87, Nos. 3–4, Dec. 1991, pp. 319–335.

[11]Yagi, S., and Iino, H., "Radiation from Soot Particles in Luminous Flames," *Eighth Symposium (International) on Combustion*, Combustion Inst., Pittsburgh, PA, 1960, pp. 288–293.

[12]Turns, S. R., *An Introduction to Combustion*, McGraw–Hill, New York, 1996, pp. 146, 291–293, 428, 480.

[13]Dagaut, P., Cathonnet, M., and Boettner, J.-C., "Kinetic Modeling of Propane Oxidation and Pyrolisis," *International Journal of Chemical Kinetics*, Vol. 24, No. 9, Sept. 1992, pp. 813–837.